

Resistance and Sub-Resistances of RC Beams Subjected to Multiple Failure Modes

F. Sangiorgio, J. Silfwerbrand, G. Mancini

Abstract—Geometric and mechanical properties all influence the resistance of RC structures and may, in certain combination of property values, increase the risk of a brittle failure of the whole system.

This paper presents a statistical and probabilistic investigation on the resistance of RC beams designed according to Eurocodes 2 and 8, and subjected to multiple failure modes, under both the natural variation of material properties and the uncertainty associated with cross-section and transverse reinforcement geometry. A full probabilistic model based on JCSS Probabilistic Model Code is derived. Different beams are studied through material nonlinear analysis via Monte Carlo simulations. The resistance model is consistent with Eurocode 2. Both a multivariate statistical evaluation and the data clustering analysis of outcomes are then performed.

Results show that the ultimate load behaviour of RC beams subjected to flexural and shear failure modes seems to be mainly influenced by the combination of the mechanical properties of both longitudinal reinforcement and stirrups, and the tensile strength of concrete, of which the latter appears to affect the overall response of the system in a nonlinear way. The model uncertainty of the resistance model used in the analysis plays undoubtedly an important role in interpreting results.

Keywords—Modelling, Monte Carlo Simulations, Probabilistic Models, Data Clustering, Reinforced Concrete Members, Structural Design.

I. INTRODUCTION

CONCRETE is the most widely used construction material in the world, and reinforced concrete (RC) structural systems are the most commonly used system in buildings and other built infrastructure. The causes that make concrete so popular between engineers and builders are due to a number of advantages that it provides over other materials such as its low cost, the workability, the durability, the incombustibility, and a comparatively high compressive strength. On the other hand, reinforced concrete is a composite, nonhomogeneous, and nonisotropic material that cracks significantly under relatively low loads, and in turns this makes it difficult to determine the strength of cracked RC members because their internal force system is not known with certainty [1], [2]; the question becomes even more complicated in the presence of shrinkage

F. Sangiorgio is Ph.D. candidate at both the Division of Structural Engineering and Bridges, KTH Royal Institute of Technology, 10044 Stockholm, Sweden, and the Department of Structural, Geotechnical and Building Engineering, Polytechnic of Turin, 10129 Turin, Italy (phone: 0046 8-790 90 47; fax: 0046 8-790 79 28; e-mail: filippo.sangiorgio@byv.kth.se and filippo.sangiorgio@polito.it).

J. Silfwerbrand and G. Mancini are professors at the Division of Structural Engineering and Bridges, KTH Royal Institute of Technology, 10044 Stockholm, Sweden, and Polytechnic of Turin, 10129 Turin, Italy, respectively (e-mail: jsilfwer@kth.se, giuseppe.mancini@polito.it).

and creep, and if we consider the redistribution of shear stresses between flexural cracks.

RC structures are brittle compared to steel structures. According to [3], flexure and shear combine to create a biaxial stress. In a region of large bending moments, these stresses are greatest at the extreme tensile fibre of the member and are responsible for the initiation of flexural cracks perpendicular to the axis of the member. In the region of high shear force, significant principal tensile stresses, also referred to as diagonal tension, may be generated on inclined planes oriented at approximately 45° to the axis of the member. Inclined cracks form when these principal tensile stresses exceed the tensile strength of concrete and, with few exceptions, they are extension of flexural cracks. Sometimes, the formation of a significant continuous diagonal crack may result in the yielding of a set of stirrups; unrestricted widening of that crack then commences, and one of the important components of shear resistance, aggregate interlock action, becomes ineffective. The shear resistance so lost cannot be transferred to the dowel and the truss mechanisms, because they are already exhausted, hence failure follows with little further deformations.

Shear failures are sudden and catastrophic in nature and should be avoided in the design process. As stated and confirmed by different researchers for a long time (e.g., [3]–[5]), since it is common practice to rely on ductile inelastic flexural response of plastic hinges to reduce the strength requirements for structures, it is important (indeed, in seismic design it is necessary) to prevent such non-ductile failure by ensuring that the shear strength exceeds the shear corresponding to maximum feasible flexural strength. This is the so-called capacity design philosophy. In this regard, our recent studies [6] and [7] have shown that the ultimate load behaviour of a RC structure designed according to Eurocodes 2 [8] and 8 [9] is not unique, but may vary from structure to structure depending upon a variety of factors (structural system, load configuration, and ductility class). The combination of those factors may lead to a preferential performance of the structure; however this seems not to affect the main failure mechanism that was demonstrated to be a ductile one. Those findings highlight that the European design specification is successful in preventing the formation of non-ductile failure mechanisms. However, nothing can be said for RC structures designed with other standards or for existing RC structures. Therefore, more investigations are needed to understand both their ultimate load behaviour and resistance.

Previous studies [10]–[13] indicated that structural resistance can be predicted by appropriate modelling of

material properties, geometry variables and uncertainties associated with the applied model. The effect of variability of materials and geometry is relatively well understood and has been extensively investigated. However, at present, there is limited information on their influence on the ultimate load behaviour of RC structures subjected to multiple failure modes (especially for the influence of uncertainties associated with both geometry and mechanical properties of stirrups). Therefore, the objective of this paper is to conduct a first in-depth study of the natural causes that may affect the ultimate load behaviour of RC beams subjected to the combination of flexural and shear failure modes, considering different structural systems, geometrical configurations, ductility classes, and diverse combinations of load actions.

The outcome of the study will be of importance for both design of new structures and assessment of existing structures where the combination of flexural and shear failure modes is the limiting aspect. A better understanding of the factors that may affect the ultimate load behaviour of RC structures will reduce safety margins without jeopardizing security. This will in turn lead to savings of natural resources.

II. THE METHODOLOGY

The method basically consists of the following five steps: (A) design procedure; (B) full probabilistic model; (C) NL-FEM analysis; (D) assessment of the model uncertainty; and (E) multivariate statistical and data clustering analysis.

A. Design Procedure

Four sets of RC beams were properly designed on the basis of linear elastic analysis for serviceability and ultimate limit states according to Eurocodes 2 and 8 for various ductility classes (Low: DCL; Medium: DCM; and High: DCH).

Samples range from a simply supported beam to unsymmetrical continuous beams. The length of the beams varies between 5 m and 15 m. Details are given in Fig. 1. For each set of RC beams, the following data are given: (i) the design load values; (ii) the structural system description; (iii) the load configuration; (iv) the ductility class; and (v) the design notation (e.g., R-30x60-2S-750-500 means a rectangular cross-section with width $b=300$ mm and depth $h=600$ mm, and two spans of 7.5 m and 5 m in length). Concrete C25/30, steel S500, and exposure class X0 were assumed. Beams were supposed to carry a typical domestic floor of 4 m width totally.

A. Full Probabilistic Model

A full probabilistic model based on JCSS Probabilistic Model Code [14], able to describe the mechanical properties of concrete and reinforcement steel, the reinforcement area, the geometrical properties of the cross-section, and the model uncertainty, was defined. Here, reinforcement is referred to as both longitudinal and transverse. Details are given in Table I. Shown in the table are (a) all the basic random variables, (b) their symbols, (c) distribution types, (d) units, (e) mean values μ , (f) standard deviations σ , (g) coefficients of variation C.o.V., and (h) coefficients of correlation ρ_{ij} . The reference to

JCSS Probabilistic Model Code [14], as reported in [15], is made because it gives guidance on the modelling of random variables in structural engineering.



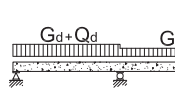

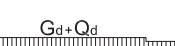

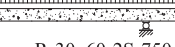

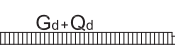

Exp. Set	Design Load [kN/m]			Structural System Description	
	G_d	Q_d			
A	31.4	12.0	L1)		-DCL
				R-30x45-1S-500-DCL-L1	
B	31.4	12.0	L1)		-DCL -DCM -DCH
			L2)		-DCL -DCM -DCH
			L3)		-DCL -DCM -DCH
				R-30x45-2S-500-500	
C	32.9	12.0	L1)		-DCL -DCM -DCH
			L2)		-DCL -DCM -DCH
			L3)		-DCL -DCM -DCH
				R-30x60-2S-750-500	
D	34.4	12.0	L1)		-DCL -DCM -DCH
			L2)		-DCL -DCM -DCH
			L3)		-DCL -DCM -DCH
				R-30x75-2S-1000-500	

Fig. 1 Design samples

For each simulation setting (designed beam), 10,000 samples were generated via the Monte Carlo method covering a wide range of mechanical and geometrical properties. The estimates were then projected at 50 years from design.

B. NL-FEM Analysis

A numerical model based on the FEM incremental-iterative nonlinear analysis of RC beams was implemented by the first author in MATLAB environment for the purpose of the present paper. The resistance model considers the combination of both flexural and shear failure mode, and is based on Eurocode 2 assumptions for RC members. Such model is certainly more complicated than the standard approach, but also more realistic.

The NL-FEM model contemplates only the material nonlinearities and is based on both the moment-curvature relation and the modified secant stiffness method [16]-[20]. The moment-curvature relationship is numerically derived using the mathematical model of the full stress-strain curves of

concrete and reinforcing steel, strain compatibility, and equilibrium equations for all the basic structural elements

composing the beam. The safety check is performed in the domain of the internal actions.

TABLE I
 PROBABILISTIC MODEL

Basic Variable	Symbol	Distr.	Unit	μ	σ	C.o.V.	Corr. Coeff. ρ_{ij}
In situ concrete compressive strength (50 years)	f_{c25}	LGN	MPa	47.82	8.20	0.17	- - -
Concrete tensile strength	f_{ct}	LGN	MPa	3.94	1.30	0.33	- - -
Bar area	A_s, A_s', A_{sw}	N	mm ²	nom. area	-	0.02	1.00 0.50 0.35
Steel yield stress	f_y, f_{yw}	N	MPa	560	30	-	0.50 1.00 0.85
Steel ultimate strength	f_u	N	MPa	$1.15 \cdot f_{y,nom}$	40	-	0.35 0.85 1.00
Dimensions of cross-section	h, b	N	mm	$0.003 \cdot X_{nom}$	$4 + 0.006 \cdot X_{nom}$	-	- - -
Concrete cover to top steel	c_s	LGN	mm	$c_{s,nom} + 10$	10	-	- - -
Effective depth of cross-section	d	N	mm	$d_{nom} + 10$	10	-	- - -
Uncertainty of resistance for bending moment (under-reinforced beams)	$\theta_{R,F}$	LGN	-	1.00	-	0.07	- - -
Uncertainty of resistance for shear	$\theta_{R,S}$	LGN	-	1.60	-	0.15	- - -

Note. N = normal distribution; LGN = lognormal distribution

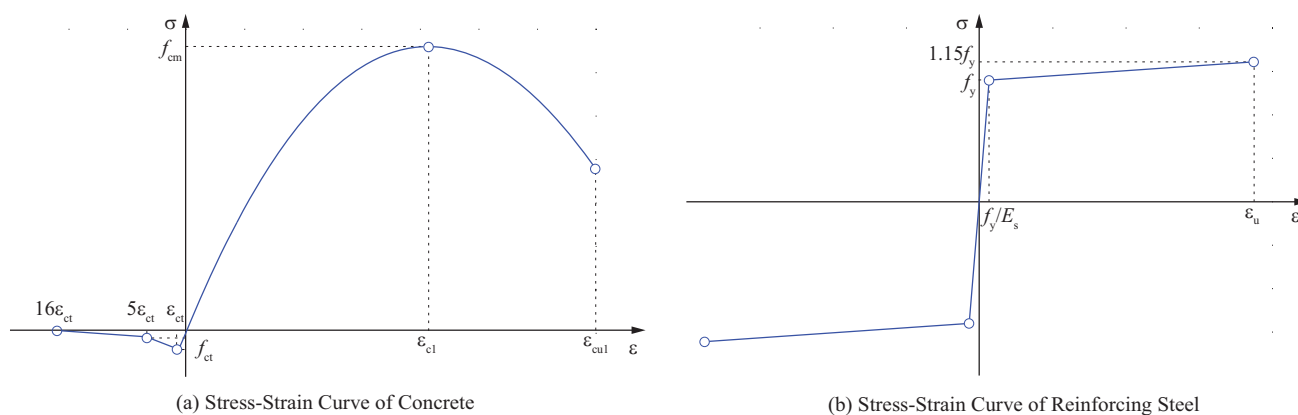


Fig. 2 Modelling of material properties

Assumptions for the analysis were as follows: (i) Bernoulli-Navier beam theory; (ii) transverse shear deformations neglected; (iii) load applied at the centroid of the cross section. Spurious sensitivity of results due to both load step and convergence criteria was reduced as follow: (a) loading was applied in a stepwise fashion with 1% increments; (b) convergence criteria were based on force and displacement, and the convergence tolerance limit was established for both calculations at 0.1%. Bond slip between steel and concrete was neglected.

The mathematical model for the stress-strain curve of concrete is shown in Fig. 2 (a). The ascending part of the curve is a parabola as proposed by Sargin [21], which is also mentioned in Eurocode 2, and represents concrete in compression, whereas concrete in tension is assumed to have a linear elastic behaviour up to the maximum tensile stress f_{ct} . After that point, tension stiffening effects are also considered according to [22]. Consistent with Eurocode 2, a bilinear stress-strain curve is utilized for reinforcing steel as shown in Fig. 2 (b). The meaning of symbols is as in the mentioned references.

C. Assessment of the Model Uncertainty

Models, descriptive or predictive, are the basic vehicles by which we reflect and express our understanding of some

aspect of reality, a particular unknown of interest. As it is virtually impossible to grasp any situation in its entire complexity, models are always partial representations of reality. In other words, what we know about the true nature of the unknown of interest is generally incomplete, resulting in a state of uncertainty. Accordingly, the uncertainties in model predictions arise from uncertainties in the values assumed by the model parameters, *parameter uncertainty*, and the uncertainties and errors associated with the structure of the model, *model uncertainty*, stemming from abstractions, assumptions, and approximations [23].

The assessment procedure for the two model uncertainties ($\theta_{R,F}$ for bending moment resistance of under-reinforced beams, and $\theta_{R,S}$ for shear resistance) went through a process of comparison with experimental results. Engineering judgment was also used. Regarding to this process, more details are given in our other work [7].

D. Multivariate Statistical and Data Clustering Analysis

The different designed beams were then analyzed up to complete loading and mechanical behaviour with the previously defined NL-FEM model. The statistical population included a total of 250,000 numerical experiments.

In safety-related checks, in the authors' opinion, it is important to explicitly define the instant of collapse (or loose

of resistance). According to Eurocode 2, in this paper collapse is referred to a limiting allowable strain in one of the basic members composing the analyzed beams corresponding to a particular limit state such as (a) crushing of concrete (assumed to occur when the strain reaches the nominal ultimate compressive strain ε_{cu1}), (b) breaking of tension reinforcements (when the strain of longitudinal rebars steel reaches the strain at maximum load ε_u), and (c) shear failure (when the strain of transverse reinforcement steel reaches the strain at yielding $\varepsilon_y=f_y/E_s$; where f_y is the yield strength of the reinforcement and E_s is its modulus of elasticity). It should be noted that the choice to assume the shear capacity exhausted when yielding of stirrups is reached is very conservative since the truss model proposed in Eurocode 2 considers the variation in the angle of the compression field θ developing in the web as a result of this yielding. For a matter of convenience, the shear checking is conducted at the force level.

Consistent with [7], for the aim of the present study, we define the sub-resistance (R_x, R_y, R_z) of a beam subjected to multiple failure modes (X, Y, Z) as the fraction of the total resistance (R) of the beam to the specific failure mechanism (e.g., flexural, shear, etc.).

The structural resistance factor λ , expressed as $\lambda=R/L_d$, where R is the resistance of the beam and L_d is the design load, was evaluated for each of the twenty-five different analyzed beams. Similarly, the structural sub-resistance factors λ_F and λ_S of the two main failure modes (flexural and shear, respectively), expressed as $\lambda_X=R_X/L_d$, where R_X is the sub-resistance of the beam related to failure mode X , were also computed.

With the intention of evaluating the influence of natural variation of both material properties and uncertainties associated with cross-section and stirrups geometry on the ultimate load behaviour of the designed beams, a multivariate statistical analysis combined with the visual exploration of the outcomes was then performed.

Additionally, data were processed by clustering using the k-means algorithm [24]-[27]. Cluster analysis divides data objects into groups (clusters) basing only on information found in the data that describe the objects and their relationship. The goal of this kind of analysis is that the objects within a group be similar (or related) to one another and different from (or unrelated to) the objects in other groups. The greater is the similarity (or homogeneity) within a group and the greater is the difference between groups, the better or more distinct is the clustering. K-means is a prototype-based (a cluster is defined as a set of objects in which each object is closer to the prototype that defines the cluster than to the prototype of any other cluster; the prototype of a cluster is often the centroid, i.e., the mean value of all the points in the cluster), partitional (simply division of the set of data objects into non-overlapping clusters) clustering technique that attempts to find a user-specified number of clusters k [28].

Clustering was performed considering parameters derived from the nonlinear analysis as the maximum bending moment (at the crucial sections) and the corresponding curvature.

Because of its simplicity, in the k-means algorithm, the use of Euclidian distance metric was preferred. The number of clusters k was chosen iteratively and heuristically. The number of repetitions of the clustering process, each with a new set of initial cluster centroid positions, was set at 250; just the solution with the lowest value for the within-cluster sums of point-to-centroid distances was considered. In order to assess the quality of the individuated clusters, the within-cluster similarities and the cluster silhouettes [29] were calculated and plotted. Conclusively, the treatment of each cluster was left to the final judgment of the authors. All the calculations were performed using the MATLAB Statistics Toolbox.

III. COMPUTATIONAL RESULTS

The cluster analysis results showed that, with respect to the flexural failure mode, the data can be further divided in (1) flexural failure with only crushing of concrete in compression zone (on average, about 10% of the total flexural failures), and (2) flexural failure with crushing of concrete and yielding of tension reinforcements (the remaining 90%). Details are omitted here.

The correlation coefficients ρ_{ij} (that in this paper will be simply denoted as r) between both the structural sub-resistance factors λ_F and λ_S of the analyzed beams and all parameters of the predictive model (width b and height h of beam, concrete cover c_s , effective depth d , compressive f_c and tensile f_{ct} strength of concrete, area of longitudinal reinforcement A_s , steel yield stress f_y and ultimate strength f_u for longitudinal bars, area of stirrups A_{sw} , steel yield stress f_{yw} for stirrups, and model uncertainties $\theta_{R,F}$ and $\theta_{R,S}$) are presented in Table II. The correlation coefficients give information on the quality of a linear relationship (linear least squares fitting) between the parameters of the problem and, therefore, on the variables that mostly influence the two sub-resistances R_F and R_S . The correlation coefficients r are also known as the product-moment coefficients of correlation or Pearson's correlations [30]. Correlations are interpreted by squaring the value of the correlation coefficients. The squared values represent the proportion of variance of one variable that can be predicted from the other variable. A rule of thumb for interpreting correlation coefficients has been established from experimental studies [31]: (i) $0.0 \leq r < 0.2$, very weak; (ii) $0.2 \leq r < 0.4$, weak; (iii) $0.4 \leq r < 0.7$, moderate; (iv) $0.7 \leq r < 0.9$, strong; and (v) $0.9 \leq r \leq 1.0$, very strong. In the table values in boldface show the most significant correlations; moreover, in order to extract valid statistical information, samples containing less than 450 records (highlighted in italics) were omitted from the statistical analysis.

Considering only the flexural failure of the beam, Fig. 3 shows the scatter plots, with both the fitting of a least squares line and the correlation coefficients r , of the flexural sub-resistance factor λ_F evaluated for beam R-30x60-2S-750-500 (experimental set C, load case L1, and DCH) versus both (a) the steel yield stress f_y and (b) the ultimate strength f_u of longitudinal bars, and (c) the model uncertainty $\theta_{R,F}$.

TABLE II – PART A
 CORRELATION COEFFICIENTS BETWEEN THE STRUCTURAL SUB-RESISTANCE FACTORS OF THE BEAMS AND ALL PARAMETERS OF THE PREDICTIVE MODEL

Exp. Set	λ_F										
	<i>b</i>	<i>h</i>	<i>c_s</i>	<i>d</i>	<i>f_c</i>	<i>f_{ct}</i>	<i>A_s</i>	<i>f_y</i>	<i>f_u</i>	$\theta_{R,F}$	
A L1)	-DCL	0.02	0.02	-0.02	0.24	0.11	0.11	0.45	0.60	0.54	0.72
	-DCL	-0.07	-0.07	0.17	0.14	-0.26	-0.44	0.08	0.17	0.17	0.54
	-DCM	-0.04	-0.04	0.13	0.12	-0.21	-0.46	0.13	0.21	0.21	0.57
B L1)	-DCH	0.03	0.03	0.05	0.10	-0.15	-0.34	0.28	0.44	0.42	0.57
	-DCL	-0.03	-0.03	0.05	0.25	-0.14	-0.23	0.27	0.46	0.42	0.73
	-DCM	0.00	0.00	0.06	0.20	-0.07	-0.18	0.32	0.46	0.42	0.71
L2)	-DCH	0.04	0.04	0.00	0.19	-0.05	-0.17	0.36	0.56	0.51	0.70
	-DCL	0.02	-0.05	0.04	0.17	-0.13	-0.20	0.31	0.51	0.50	0.69
	-DCM	0.04	-0.09	0.10	0.24	-0.13	-0.24	0.23	0.32	0.32	0.58
L3)	-DCH	-0.02	-0.02	-0.03	0.20	-0.07	-0.22	0.30	0.48	0.46	0.70
	-DCL	0.04	0.03	-0.03	0.19	0.03	-0.04	0.44	0.53	0.48	0.77
	-DCM	-0.01	0.01	-0.04	0.18	0.00	-0.03	0.37	0.48	0.45	0.72
C L2)	-DCH	0.00	0.05	-0.07	0.15	0.00	-0.09	0.34	0.54	0.50	0.74
	-DCL	0.06	0.00	0.01	0.23	-0.10	-0.24	0.32	0.44	0.38	0.65
	-DCM	0.15	-0.03	-0.14	0.35	0.08	-0.11	0.40	0.29	0.26	0.62
L3)	-DCH	0.05	-0.12	0.08	0.18	-0.18	-0.45	0.05	0.24	0.23	0.65
	-DCL	-0.03	0.03	-0.01	0.10	-0.13	-0.18	0.34	0.52	0.48	0.70
	-DCM	0.01	-0.04	-0.02	0.19	-0.07	-0.12	0.29	0.42	0.40	0.73
L1)	-DCH	-0.01	-0.05	0.02	0.11	0.00	-0.14	0.36	0.54	0.49	0.75
	-DCL	-0.01	0.02	-0.05	0.10	-0.07	-0.03	0.35	0.49	0.44	0.74
	-DCM	0.03	0.00	0.00	0.21	0.00	-0.10	0.36	0.50	0.46	0.78
D L2)	-DCH	0.00	0.01	-0.06	0.11	0.03	-0.06	0.34	0.52	0.47	0.75
	-DCL	0.06	-0.04	0.03	0.07	-0.28	-0.25	0.21	0.35	0.29	0.55
	-DCM	0.04	-0.15	0.10	0.22	-0.04	-0.15	0.26	0.28	0.24	0.66
L3)	-DCH	0.03	-0.05	0.03	0.19	-0.03	-0.26	0.27	0.42	0.42	0.71

TABLE II – PART B
 CORRELATION COEFFICIENTS BETWEEN THE STRUCTURAL SUB-RESISTANCE FACTORS OF THE BEAMS AND ALL PARAMETERS OF THE PREDICTIVE MODEL

Exp. Set	λ_S									
	<i>b</i>	<i>h</i>	<i>c_s</i>	<i>d</i>	<i>f_c</i>	<i>f_{ct}</i>	<i>A_{sw}</i>	<i>f_{yw}</i>	$\theta_{R,S}$	
A L1)	-DCL	0.00	0.01	0.14	0.17	0.15	0.23	-0.08	-0.15	0.88
	-DCL	-0.02	-0.02	0.01	0.16	-0.03	-0.01	0.26	0.38	0.90
	-DCM	0.01	0.01	-0.01	0.14	-0.01	-0.02	0.24	0.33	0.89
B L1)	-DCH	0.03	0.03	0.01	0.08	-0.01	0.07	0.17	0.23	0.89
	-DCL	-0.02	-0.02	0.02	0.16	-0.01	-0.03	0.26	0.35	0.90
	-DCM	0.00	0.00	0.01	0.15	-0.02	-0.02	0.24	0.34	0.91
L2)	-DCH	0.03	0.03	0.02	0.11	0.01	0.02	0.17	0.26	0.92
	-DCL	-0.01	-0.02	0.04	0.13	-0.01	-0.01	0.24	0.36	0.91
	-DCM	0.00	-0.03	0.05	0.17	-0.02	-0.02	0.27	0.36	0.90
L1)	-DCH	-0.01	-0.04	0.02	0.14	0.00	0.01	0.24	0.35	0.91
	-DCL	-0.01	0.00	0.03	0.12	0.00	-0.01	0.26	0.35	0.92
	-DCM	-0.01	-0.01	0.01	0.13	0.01	0.00	0.26	0.35	0.91
C L2)	-DCH	0.01	-0.01	0.01	0.12	0.02	0.01	0.21	0.31	0.93
	-DCL	-0.01	0.00	0.03	0.10	-0.02	0.02	0.27	0.38	0.90
	-DCM	-0.01	-0.04	0.05	0.17	-0.01	-0.02	0.28	0.38	0.89
L3)	-DCH	-0.02	-0.04	0.05	0.18	-0.01	-0.01	0.29	0.38	0.89
	-DCL	0.00	-0.01	-0.01	0.10	0.05	0.03	0.15	0.25	0.91
	-DCM	0.00	-0.01	0.00	0.12	0.03	0.01	0.27	0.35	0.92
L1)	-DCH	0.01	-0.02	0.01	0.12	0.01	0.01	0.23	0.33	0.92
	-DCL	0.02	0.00	0.00	0.10	0.04	0.03	0.18	0.25	0.92
	-DCM	0.00	-0.02	0.01	0.12	0.03	0.01	0.26	0.35	0.92
D L2)	-DCH	0.00	-0.02	-0.02	0.10	0.02	0.02	0.23	0.32	0.93
	-DCL	0.00	-0.02	0.03	0.10	0.00	-0.01	0.26	0.36	0.91
	-DCM	0.00	-0.07	0.00	0.15	0.03	0.02	0.26	0.36	0.90
L3)	-DCH	0.00	-0.02	0.02	0.11	0.00	0.01	0.24	0.33	0.92

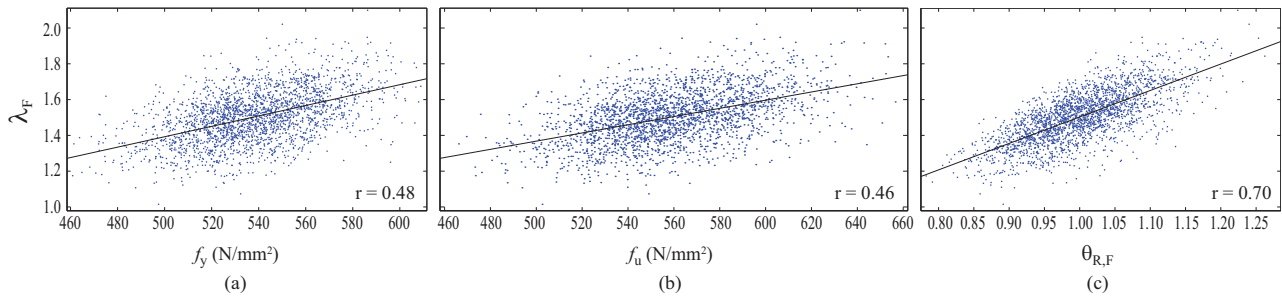


Fig. 3 Scatter plots, with both fitting of a least squares line and correlation coefficients r , of the flexural sub-resistance factor λ_F for beam R-30x60-2S-750-500 (experimental set C, load case L1, and DCH) plotted versus both (a) the steel yield stress f_y and (b) the ultimate strength f_u of longitudinal bars, and (c) the model uncertainty $\theta_{R,F}$

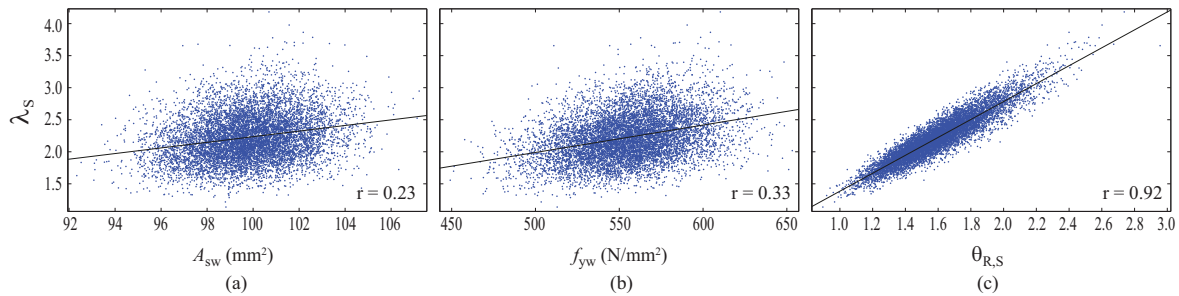


Fig. 4 Scatter plots, with both fitting of a least squares line and correlation coefficients r , of the shear sub-resistance factor λ_S for beam R-30x75-2S-1000-500 (experimental set D, load case L1, and DCH) plotted versus (a) the area of stirrups A_{sw} , (b) the steel yield stress f_{yw} of the stirrups, and (c) the model uncertainty $\theta_{R,S}$

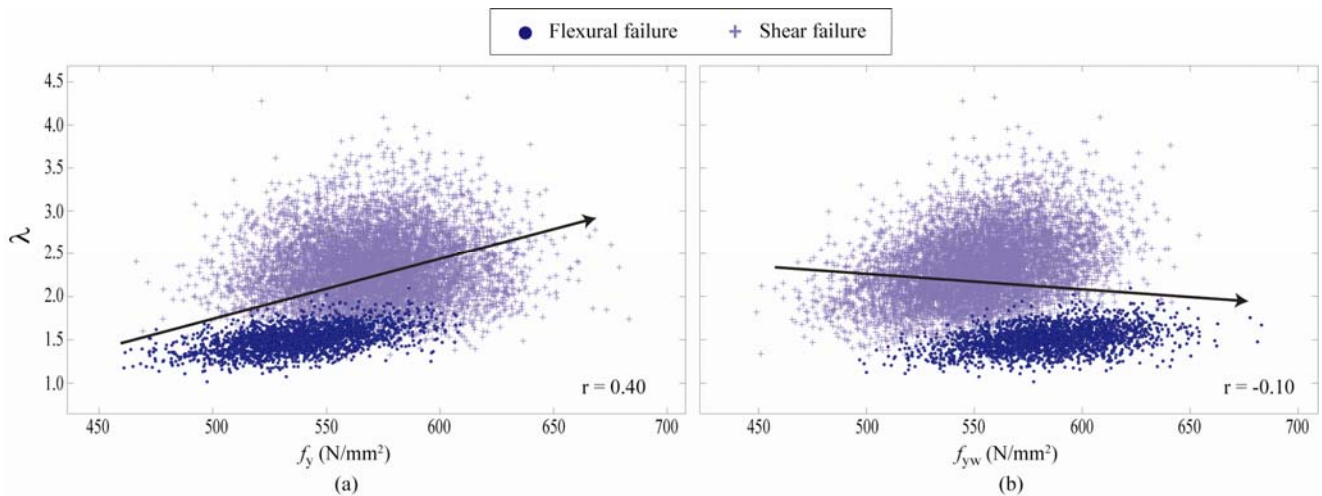


Fig. 5 Scatter plots of the structural resistance factor λ evaluated for beam R-30x60-2S-750-500 (experimental set C, load case L1, and DCH) plotted versus the steel yield stress of both (a) the longitudinal bars f_y and (b) the stirrups f_{yw} , and grouped by failure mode (flexural and shear)

Again, considering only the shear failure of the beam, Fig. 4 shows the scatter plots, with both the fitting of a least squares line and the correlation coefficients r , of the shear sub-resistance factor λ_S evaluated for beam R-30x75-2S-1000-500 (experimental set D, load case L1, and DCH) versus (a) the area of stirrups A_{sw} , (b) the steel yield stress f_{yw} of the stirrups, and (c) the model uncertainty $\theta_{R,S}$.

Fig. 5 shows the scatter plots of the structural resistance factor λ evaluated for again beam R-30x60-2S-750-500 versus the steel yield stress of both (a) the longitudinal bars f_y and (b) the stirrups f_{yw} , and grouped by failure mode (flexural and

shear).

Similarly, the scatter plots of the structural resistance factor λ evaluated for beam R-30x45-2S-500-500 (experimental set B, load case L1, and DCM) as function of both (a) the compressive f_c and (b) the tensile f_{ct} strength of concrete is displayed in Fig. 6. Here, data are again grouped by failure modes. In addition, taking the estimates given by the clustering analysis, in Fig. 6b the data related to the flexural failure mode are further divided in (1) crushing of concrete, and (2) crushing of concrete with yielding of tension reinforcements.

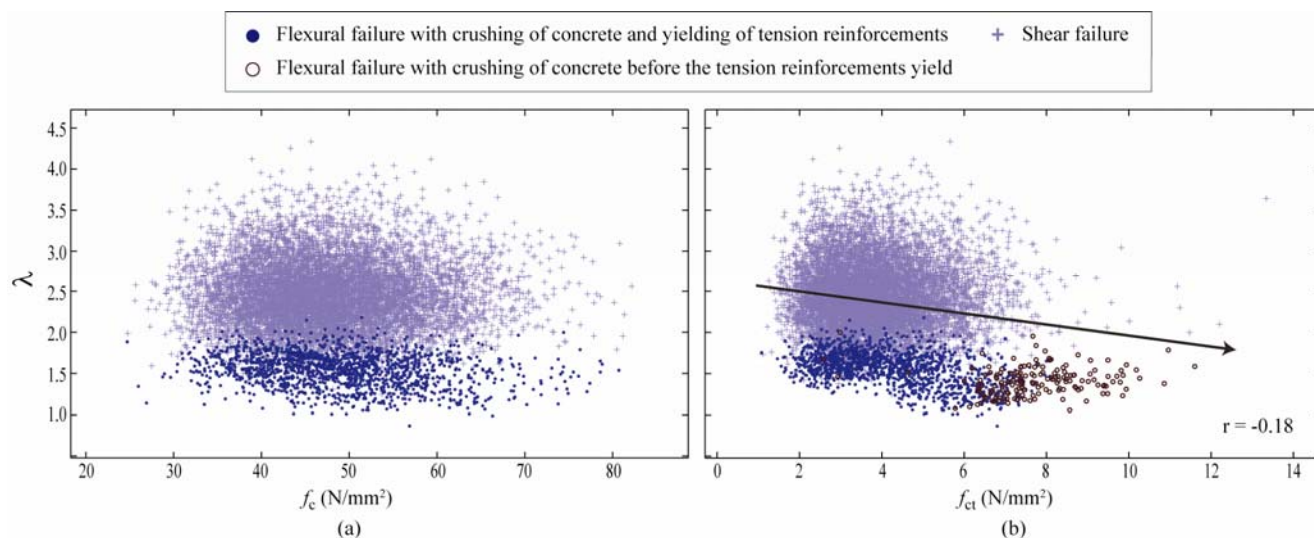


Fig. 6 Scatter plots of the structural resistance factor λ evaluated for beam R-30x45-2S-500-500 (experimental set B, load case L1, and DCM) plotted versus both (a) the compressive f_c and (b) the tensile f_{ct} strength of concrete

Furthermore, regarding again beam R-30x45-2S-500-500, Fig. 7 shows the moment-curvature relationships (in absolute values) for the cross-section over the internal support depending on the values of the tensile strength of concrete f_{ct} . The cross section has width $b = 300$ mm, height $h = 450$ mm, concrete cover $c_s = 40$ mm, and effective depth $d = 410$ mm. Mechanical properties of concrete and reinforcing steel are as follows: (i) compressive strength of concrete $f_c = 60$ N/mm²; (ii) tensile strength of concrete f_{ct} in the range 3-12 N/mm²; (iii) steel yield stress $f_y = 560$ N/mm²; and (iv) steel ultimate stress $f_u = 1.15 f_y$.

IV. DISCUSSION

In the authors' opinion, it is noteworthy to highlight the importance of using supplementary information like scatter plots before interpreting correlation coefficients. The correlation coefficient is, in fact, a numerical summary and, as such, it can be reported as a measure of association for any batch of numbers, no matter the data structure [32].

Therefore, an examination of Table II (both parts A and B) in conjunction with both Figs. 3 and 4 reveals, within the limits of our study, the following main features.

- (i) The model uncertainties ($\theta_{R,F}$ and $\theta_{R,S}$) undoubtedly affect the predictions of the NL-FEM model. There is a strong positive correlation shown by a Pearson coefficient of about 0.70 and 0.91 (average values over the all experimental sets), respectively, that cover almost the 49 and 83 percent of the total variation of the two structural sub-resistance factors, λ_F (for flexural failure) and λ_S (for shear failure).
- (ii) The steel yield stress f_y and the ultimate strength f_u of the longitudinal bars seem to be moderately correlated with the flexural sub-resistance factor λ_F . The coefficients of correlation are approximately 0.46 and 0.43, respectively,

and cover, in this case, the 21% and 18% of the total variation of the sub-resistance factor.

- (iii) A weak positive correlation is visible between λ_S and both the area A_{sw} and the steel yield stress f_{yw} of stirrups, with coefficients of correlation of around 0.23 and 0.33, respectively, that cover only the 5 and 11 percent of the total variation of the examined sub-resistance factor. However, due to the strong influence of $\theta_{R,S}$, this relationship appears to be of little relevance to the engineering aspects.

An analysis of both Figs. 5 and 6 shows at first sight that shear failure occurs at higher λ than flexural failure. That means that, in average, flexural failure occurs before shear failure, and an overall ductile behaviour is expected for the designed structures.

Moreover, as can be seen from Fig. 5 (the arrows represent the linear regression trend line), the mechanical properties of both longitudinal reinforcement and stirrups affect, somehow, the ultimate load behaviour of RC beams subjected to flexural and shear failure modes. An increase of the steel yield stress f_y of the longitudinal bars seems, in fact, to lead preferably to a shear failure and, consequently, to a brittle behaviour of the structure, whereas an increase of the steel yield stress f_{yw} of stirrups seems to conduct to a preferential flexural failure and, accordingly, to an improvement of the structural ductility. It should be noted that the vice-versa can also be performed (reinforcing steel is very ductile both in tension and compression) but only provided local instability (local buckling) due to buckling of bars is prevented.

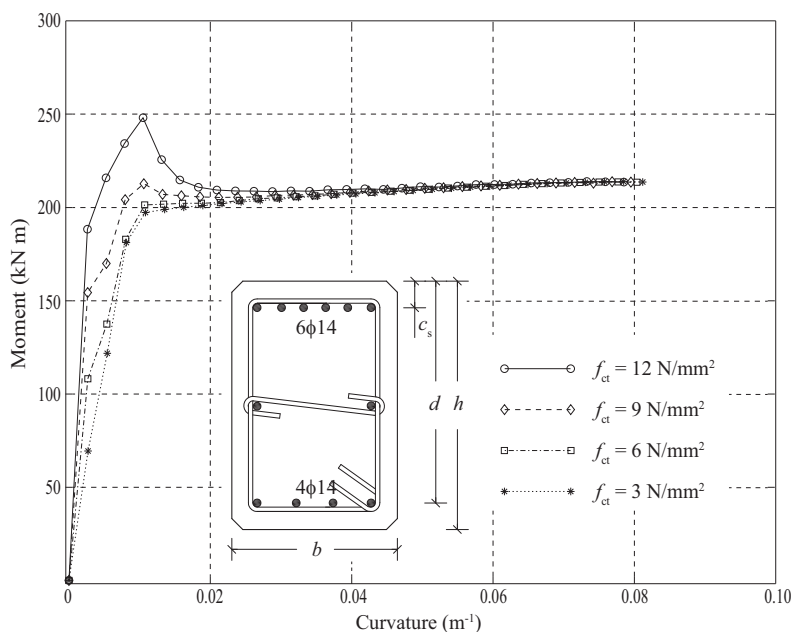


Fig. 7 Moment-curvature relationships (in absolute values) for the cross-section over the internal support of beam R-30x45-2S-500-500 (experimental set B, load case L1, and DCM) depending on the tensile strength of concrete f_{ct}

Whilst on this topic, an analysis of Fig. 6 (a) reveals, additionally, that the compressive strength of concrete f_c does not, or very weakly, affect neither the structural failure mode nor the structural resistance factor λ . On the other hand, from Fig. 6 (b) (here again the arrow represents the linear regression trend line) it is possible to see a weak nonlinear relationship between the tensile strength of concrete f_{ct} and the ultimate load behaviour of the RC beam (the data have a pronounced nonlinear structure). In this case, in fact, an increase of f_{ct} seems to induce a flexural brittle failure by crushing of the compressive concrete before the tension steel yields, which does not provide any warning before failure as the failure is instantaneous (apparent over-reinforcement of the beam).

A better understanding of the data in Fig. 6 (b) may be also obtained by considering the moment-curvature relationships displayed in Fig. 7 where an high value of f_{ct} (e.g., between 9 and 12 N/mm²) is shown to lead to a brittle failure of the cross-section with crash of concrete in compression before the tension steel yields (given by the peak of the curve).

Finally, as can be interpreted from Table II (both parts A and B), a negligible correlation is seen between both λ_F and λ_S and the other parameters ($r < 0.20$ in average value).

V. CONCLUDING REMARKS

In summary, the natural causes that affect the ultimate load behaviour of RC beams designed according to Eurocodes 2 and 8 considering different structural systems, geometrical configurations and ductility classes, and subjected to the combination of flexural and shear failure modes, under diverse combinations of load actions, were in-depth studied in a statistical-probabilistic way, and with the aid of data clustering techniques.

Due to the complexity of the challenge, an extensive use of

mathematical models and numerical methods, in combination with experimental observations, was made. In this regard, a NL-FEM model, based on Eurocode 2 assumptions for members subjected to the combination of flexure and shear, was proposed by the first author. The JCSS Probabilistic Model Code was used as source for the stochastic modelling.

As a result, within the limits of our study, it has been shown that the ultimate load behaviour of RC beams subjected to flexural and shear failure modes seems to be mainly influenced by the combination of the mechanical properties of both longitudinal reinforcement and stirrups. An increase of the steel yield stress f_y of the longitudinal bars seems, in fact, to lead preferably to a shear failure and, consequently, to a brittle behaviour of the structure, whereas an increase of the steel yield stress f_{yw} of stirrups seems to conduct to a preferential flexural failure and, accordingly, to an improvement of the structural ductility. It should be noted that the vice-versa can also be performed (reinforcing steel is very ductile both in tension and compression) but only provided local instability (local buckling) due to buckling of bars is prevented.

Tensile strength of concrete, on the other hand, appears to slightly affect the overall response of the system in a nonlinear way. Indeed, an increase of f_{ct} seems to induce a flexural brittle failure by crushing of the compressive concrete before the tension steel yields (which does not provide any warning before failure) and, in turn, may reduce the overall resistance of the structure by preventing the redistribution of bending moments. The model uncertainty of the resistance model used in the analysis plays undoubtedly an important role in interpreting results. More studies on more cases and different structural systems are needed to confirm these results.

These findings will be of importance for researchers

interested in both design of new structures and assessment of existing structures where the combination of flexural and shear failure modes is the limiting aspect. A better understanding of the factors that affect the ultimate load behaviour of RC structures will reduce safety margins without jeopardizing security. This will in turn lead to savings of natural resources.

Finally, it is pointed out that the designs of the tested beams are provided to interested researchers by contacting the first author of the paper.

REFERENCES

- [1] W.J. Krefeld, C.W. Thurston, "Contribution of Longitudinal Steel to Shear Resistance of Reinforced Concrete Beams," *ACI Journal* 63, No. 3, 1966, pp. 325-344.
- [2] W.J. Krefeld, C.W. Thurston, "Studies of the Shear and Diagonal Tension Strength of Simply Supported Reinforced Concrete Beams," *ACI Journal* 63, No. 4, 1966, pp. 451-476.
- [3] R. Park, T. Paulay, "Reinforced Concrete Structures," New York: WILEY, 1975.
- [4] B.G. Ang, M.J.N. Priestley, T. Paulay, "Seismic Shear Strength of Circular Reinforced Concrete Columns," *ACI Struct. J.* 86, No. 1, 1989, pp. 45-59.
- [5] M.J.N. Priestley, V. Ravindra, X. Yan, "Seismic Shear Strength of Reinforced Concrete Columns," *ASCE Journal of Structural Engineering* 120, No. 8, 1994, pp. 2310-2329.
- [6] F. Sangiorgio, J. Silfwerbrand, G. Mancini, "Statistical Investigation on the Ultimate Load Behaviour of RC Beams Subjected to Multiple Failure Modes," *Nordic Concrete Research* 50, 2014, pp. 457-460.
- [7] F. Sangiorgio, J. Silfwerbrand, G. Mancini, "Probabilistic Investigation of the Ultimate Load Behaviour of RC Structures Designed According to EN 1992-1-1 and Subjected to Multiple Failure Modes," *Engineering Structures*, submitted for publication.
- [8] Eurocode 2 (EN 1992-1-1), "Design of concrete structures. Part 1-1: general rules and rules for buildings," 2004.
- [9] Eurocode 8 (EN 1998-1), "Design of structures for earthquake resistance," 1998.
- [10] G. Bertagnoli, L. Giordano, G. Mancini, "Safety Format for the Nonlinear Analysis of Concrete Structures. Studi e ricerche," *Politecnico di Milano, Scuola di specializzazione in costruzioni in cemento armato* 25, 2004, pp. 31-56.
- [11] V. Červenka, "Global Safety Format for Nonlinear Calculation of Reinforced Concrete," *Beton und Stahlbetonbau* 103, 2008, pp. 37-42.
- [12] H. Schulne, M. Plos, K. Gylltoft, "Safety Formats for Nonlinear Analysis Tested on Concrete Beams Subjected to Shear Forces and Bending Moments," *Eng. Struct.* 33, No. 8, 2011, pp. 2350-2356.
- [13] M. Sykora, M. Holicky, "Safety Format for Non-Linear Analysis in the Model Code - Verification of Reliability Level," *Fib Symposium on Concrete engineering for excellence and efficiency*, Prague, Czech Concrete Society, 2011, pp. 943-946.
- [14] Joint Committee on Structural Safety, "Probabilistic Model Code 2000," JCSS-OSTL/DIA/VROU-10-11-2000.
- [15] T. Vrouwenvelder, "Reliability Based Code Calibration. The Use of the JCSS Probabilistic Model Code," *Joint Committee of Structural Safety Workshop on Code Calibration*, 2002, March 21/22, Zurich.
- [16] J.K. Kim, T.G. Lee, "Nonlinear Analysis of Reinforced Concrete Beams with Softening," *Computer and structures* 44, No. 3, 1992, pp. 567-573.
- [17] H.A.S. Rasheed, K.S. Dinno, "An Efficient Nonlinear Analysis of RC Sections," *Computers and Structures* 53, No. 3, 1994, pp. 613-623.
- [18] H.A.S. Rasheed, K.S. Dinno, "An Improved Nonlinear Analysis of Reinforced Concrete Frames," *Computers and Structures* 53, No. 3, 1994, pp. 625-636.
- [19] H.G. Kwak, S.P. Kim, "Nonlinear analysis of RC beams based on moment-curvature relation," *Computer and structures* 80, 2002, pp. 615-628.
- [20] H.R. Valipour, S.J. Foster, "A Total Secant Flexibility-Based Formulation for Frame Elements with Physical and Geometrical Nonlinearities," *Finite Elements in Analysis and Design* 46, 2010, pp. 288-297.
- [21] M. Sargin, "Stress-Strain Relationships for Concrete and the Analysis of Structural Concrete Sections," University of Waterloo, Solid Mechanics Division, SM Study 4, 1971, pp. 23-46.
- [22] B. Massicotte, A.E. Elwi, J.G. MacGregor, "Tension-Stiffening Model for Planar Reinforced Concrete Members," *ASCE J. Struct. Eng.* 116, vol. 11, 1990, pp. 3039-3058.
- [23] E.L. Droggett, A. Mosleh, "Bayesian Methodology for Model Uncertainty Using Model Performance Data," *Risk Analysis* 28, No. 5, 2008, pp. 1457-1476.
- [24] J.B. MacQueen, "Some Methods for Classification and Analysis of Multivariate Observations," *Proceedings of the 5th Berkeley Symposium on Mathematical Statistics and Probability*, 1967, pp. 281-297.
- [25] M.R. Anderberg, "Cluster Analysis for Applications," *Academic Press*, 1973.
- [26] A.K. Jain, R.C. Dubes, "Algorithms for Clustering Data," *Prentice Hall*, 1988.
- [27] L. Kaufman, P.J. Rousseeuw, "Finding Groups in Data - An Introduction to Cluster Analysis," *Wiley*, 1990.
- [28] P.N. Tan, M. Steinbach, V. Kumar, "Introduction to Data Mining," *Addison-Wesley*, 2006.
- [29] P.J. Rousseeuw, "Silhouettes: A Graphical Aid to the Interpretation and Validation of a Cluster Analysis," *J Comput Applied Math* 20, 1987, pp. 53-65.
- [30] G.W. Snedecor, W.G. Cochran, "Statistical Methods," 6th ed. Iowa State Univ. Press, Ames, 1967.
- [31] E. Garcia, "A Tutorial on Correlation Coefficients," <http://www.miislita.com>, 2010 - simmons.edu.
- [32] G.E. Dallal, "Correlation Coefficients," <http://www.jerrydallal.com/LHSP/corr.htm>, 1999.